THE PAST AND PRESENT OF A SUBSTELLAR COMPANION IRRADIATED BY A WHITE DWARF

Daphne Broski-Laing
Affiliation: University of Virginia – Advisor: Yifan Zhou

Short-period white dwarf-brown dwarf binaries (WD–BDs) are unique laboratories of substellar atmospheres. Tidally locked by the white dwarf, the brown dwarf is governed by dynamic atmospheric processes resembling those in hot Jupiters. Their unique formation histories provide a glimpse into planetary systems of post-main-sequence stars. We present the first *JWST* WD–BD phase curve, a NIRSpec PRISM observation of ZTFJ0038+2030. We obtain a full-orbit phase curve, including a total eclipse of the white dwarf, which enables us to separate the white dwarf and brown dwarf's emission throughout the entire orbit. The PRISM spectrum covers $\sim$90% of the brown dwarf's bolometric emission, enabling a nearly model-independent energy balance calculation, which yields a day-to-nightside heat redistribution efficiency of $\lesssim 10\%$. Inefficient circulation in the brown dwarf's atmosphere is further supported by the phase curve shape and the nightside emission spectrum, which closely resembles non-irradiated mid-to-late T dwarfs. The brown dwarf modulation is symmetric in the entire wavelength coverage except for the wavelengths associated with a strong CO_2 absorption feature at 4.2 μm, which reveals a stark nightside asymmetry. The precise internal luminosity measurement of the brown dwarf constrains both the age of the WD–BD system (7.4-8.8 Gyr) and a low common-envelope efficiency. These data illustrate the exquisite opportunity to probe the three-dimensional processes of substellar atmospheres, connect substellar and exoplanet atmospheres, and probe the evolution of post-main-sequence planetary systems using WD–BDs.

Research Overview

Over the past few semesters, my research has focused on the JWST observations of ZTF0038, the first WD-BD observed with JWST. We observed a full-orbit spectroscopic phase-curve of ZTF0038 throughout its 10 hour period. We observe the near-infrared spectrum from 0.6-5.3 μm. This binary is separated by $\sim$ 2 $R_\odot$, the brown dwarf's radius is $0.76R_{Jup}$, and the white dwarf's radius is $0.14R_{Jup}$.

My first task for this project was to create a data-processing pipeline that produces high-quality, absolute-calibrated time series spectra. I did most of the work for this pipeline during my first semester of graduate school (Fall 2024), and I implemented several improvements throughout the spring of 2025. This pipeline is being used for several other time-series observations of brown dwarfs. In my spectral extraction pipeline, I utilize both the standard `jwst` pipeline (Bushouse et al., 2023) as well as `Eureka!` (Bell et al., 2022) to generate a single set of wavelength-dependent calibration factors that are applied uniformly to each spectrum in the observation. In December of 2024, ZTF0038 was observed with JWST, and I ran the data through this pipeline.

The following semester, during the spring of 2025, I analyzed the data and refined the data processing pipeline. I took advantage of the eclipsing geometry in order to empirically separate the brown dwarf emission from the white dwarf signal. I prepared 8 'representative' spectra of the brown dwarf at 8 points throughout the orbit (see the lower right panel of Figure 1). Over the past year as a VSGC Graduate Research Fellow, I have been leading the analysis of the ZTF0038 phase curves. Now that I have drafted the paper, I will discuss the analysis that leads to the two main focuses of the paper: 1) the present energy transport across the brown dwarf's atmosphere, and 2) the past (post-main sequence) evolution of the system.

Energy Transport in ZTF0038B

One of the key fidings from my research over this past year is that **ZTF0038B experiences very inefficient heat transport across the brown dwarf's atmosphere.** This is evident in my energy balance calculation, the phase curve shape, and the nightside spectrum.

Energy Balance Calculation:
I carried out a simple and (almost) model-independent energy balance calculation to determine the energy transport efficiency directly. In order to do this, I first calculated the bolometric dayside and nightside luminosity of the brown dwarf. I integrated the spectra across the entire wavelength coverage to calculate the total observed day and nightside spectra. Although most of the brown dwarf's emission is captured within PRISM's wavelength coverage, a bolometric correction factor is necessary to calculate the bolometric flux of the brown dwarf. I calculate bolometric corrections using model spectra with coverage well into the mid-IR (20+ μm). For the model, I calculate how much of the total flux is covered in the PRISM wavelength coverage (from 0.6 - 5.3 μm). We assume that the observed spectrum covers the same proportion of the bolometric flux.

I used forward model fits for the day and nightside emission to calculate separate bolometric correction factors for each side. The nightside spectrum is fit using a spectral fitting tool (`species`, Stolker et al. (2020)) that interpolates the Sonora Bobcat model grid (Marley et al., 2021) and implements nested sampling to fit the spectrum. The dayside is fit using a grid of irradiated substellar atmosphere models (Mayorga et al., 2021). In order to provide a range of plausible luminosities, I estimate a range of plausible bolometric correction factors using a range of model fits 'centered' around the best-fit parameters. I'm still developing the final procedure to do this more robustly, but an initial implementation is shown in Figure 2, where the yellow dashed line shows an implementation assuming a smaller bolometric correction for both the day and nightside, and the pink dashed line shows the implementation with a large bolometric correction.

Using the measured bolometric luminosities of the brown dwarf's dayside and nightside (with appropriate bolometric corrections), I constrain several key components of its energy budget. First, the internal luminosity (L_{int}) represents the brown dwarf's internal heat, independent of irradiation from the white dwarf. L_{int} is the total observed emission from both hemispheres minus the absorbed stellar energy:

$$L_{\text{int}} = L_{\text{bol, day}} + L_{\text{bol, night}} - L_{\text{irr}}. \quad (1)$$

The irradiation luminosity (L_{irr}) corresponds to the stellar energy absorbed by the brown dwarf from the white dwarf. This depends on the incident flux (F_{incident}), the radius of the brown dwarf (R_{BD}), and the Bond albedo (A):

$$L_{\text{irr}} = (1 - A) \cdot F_{\text{incident}} \cdot \pi R_{\text{BD}}^2. \quad (2)$$

Some of L_{irr} is circulated from the dayside to the nightside. We define this transported energy as L_{cir}, which we calculate as the nightside

luminosity minus half the internal luminosity. Based on the energy balance of the nightside, L_{cir} can be expressed as:

$$L_{\text{cir}} = L_{\text{night}} - \frac{L_{\text{int}}}{2}. \quad (3)$$

We divide L_{int} by two because the nightside luminosity represents one hemisphere, while L_{int} represents the emission from entire brown dwarf.

We define the heat transport efficiency (ϵ), which quantifies the amount of the energy absorbed from the white dwarf that is ciculated to the nightside:

$$\epsilon = \frac{L_{\text{cir}}}{L_{\text{irr}}}. \quad (4)$$

These calculations constrain the internal luminosity and energy transport efficiency as a function of albedo. We calculate these values for three scenarios using different bolometric correction estimates: 1) best-fit values, 2) upper estimates, and 3) lower estimates, as shown in Figure 2. Our JWST observations cover around 88% of the bolometric flux of the brown dwarf, making these energy budget calculations among the most thorough energy budgets of any irradiated substellar atmosphere outside of our solar system (Splinter et al., 2025).

Phase Curve Shape:

Another piece of evidence supporting low energy transport efficiency is the phase curve shape. As seen in Figure 1, the maximum point of the phase curve is somewhat 'peaked', while the troughs are flat. This is quantitatively verified by the fact that the phase curve is best-fit with a second order Fourier series. This shape is not caused by deformation of the brown dwarf (because the effect would actually diminish the 'peakiness' observed in ZTF0038's phase curve). Instead, this shape may be caused by a hotspot located at the substellar point, directly facing the white dwarf host. This implies that the heat is received at this substellar point, and it is not being efficiently redistributed across the atmosphere. Additionally, it is notable that the peak is centered *directly* at the 0.5 phase, which corresponds exactly to the substellar point. If there was an offset (like is commonly seen in hot Jupiter atmospheres), the offset would be indicative of equatorial jets that cause the hotspot to be located eastward of the substellar point (typically).

I also note that there is a peculiar lightcurve asymmetry found around 4.3 μm, a strong CO_2 feature. This is seen (faintly) in Figure 1. I plan to discuss this feature with our team this month, but it is possible that this feature presents the first observational evidence of pressure-dependent heat redistribution in a substellar atmosphere.

Recognizable Nightside Spectrum:

The emission of ZTF0038B shares features that are familiar to isolated brown dwarf spectra. In my paper, I fit the day and nightside spectra with non-irradiated brown dwarf models, and I compare the nightside spectrum with isolated brown dwarf spectra observed with JWST. Because the nightside spectrum still behaves much like non-irradiated brown dwarfs, this further supports our claim that very little heat is redistributed from the irradiated dayside to the nightside.

The History of ZTF0038B

In addition to the new constraints on the atmospheric behavior of ZTF0038B, we also discuss the history and evolution of the system. Our primary takeaways are that the binary has a **stable period**, it **does not show signs of excess heat from the common-envelope phase**, and it now has a **well-constrained age**.

Eclipse Timing:

I fit the eclipse profile using `batman` (Kreidberg, 2015) (see Figure 1), and compared the eclipse timing with published results from the

discovery paper (van Roestel et al., 2021). This constrained the period with a precision of 60μs, and indicates that system is in a stable orbit. For this reason, I assume that gravitational radiation negligible for this system, and it doesn't appear that there are other angular momentum effects that are noticeably removing angular momentum from the system.

No Excess Heat from the CEE Phase:

In the bottom panel of Figure 2, I compare the internal luminosity of the brown dwarf (internal luminosity is the luminosity contribution from the internal heat, not the energy from the irradiation) to isolated brown dwarf evolutionary tracks. Zorotovic & Schreiber (2022) present a range of viable progenitor masses with associated main sequence lifetimes between 2.2 - 8.8 Gyr. With our new luminosity constraints, we require that the luminosity must be *at least* as large as the evolutionary model predicts, because the model is our lower limit for this brown dwarf's true age. This is because the brown dwarf may have been heated by the white dwarf, but there are no proposed mechanisms for accelerated cooling of brown dwarfs in WD-BDs. Using this logic, we have two conclusions. Firstly, the age is now constrained to be between 7.5 - 8.8 Gyr (as opposed to a proposed range of 2.2 - 8.8 Gyr). Secondly, we are able to provide more robust constraints on the common-envelope efficiency, $\alpha_{\rm CE}$. In practice, we can see from Figure **??** that our age constraints would not greatly impact the range of allowed $\alpha_{\rm CE}$ values shown in blue. However, the age cutoff used to select the blue range of values was much less reliable than the age limits we report. Compared to the gray $\alpha_{\rm CE}$ values shown, our age constraints greatly improve the range of allowed $\alpha_{\rm CE}$. We would need to re-run the methods of Zorotovic & Schreiber (2022) to produce a precise range of allowed efficiencies, but it is clear from the figure that our constraints would produce constraints similar to those found with the age restriction implemented in the paper ($0.24 < \alpha_{\rm CE} < 0.43$).

Future Research Trajectory

My immediate next step is fairly straightforward. I'm heavily involved in the analysis of WD-BDs from the JWST program #4967, which observed 5 WD-BD phase curves. I will carry out a similar analysis of another WD-BD, WD0137. Then, once all members of our collaboration complete the analysis of the remaining 3 objects, I will lead a paper synthesizing the results from all 5 observations. After this, I have a few ideas of the directions that I could pursue as I work toward my PhD. Which projects I end up working on will depend on the success of JWST observing proposals, and our findings from our sample of WD-BDs. In the following section, I will discuss some potential directions of my PhD research trajectory.

Analysis of WD 0137: This object has a shorter period, higher level of irradiation, and it is not eclipsing. Compared to ZTF0038, I will investigate similar properties in this system, but it will present additional complications that make its analysis exciting and instructional for my own learning and growth. These phase curves do not include an eclipse, which means that it will be a bit trickier to separate the brown dwarf signal from the white dwarf signal. Additionally, this object is much more extreme than ZTF0038; it rotates much faster than ZTF0038 and it receives much stronger irradiation. I anticipate that WD0137 will push our current substellar models to their limits - even more so than ZTF0038. Additionally, because of WD0137B's proximity to the white dwarf host, it is more likely that WD 0137 will show signs of excess heat as a result of the common-envelope phase (as discussed in Zorotovic & Schreiber (2022)). This complicates our ability to constrain the age of the system. In our observation of ZTF0038, the internal heat is used to constrain the age, and we find it un-

likely that this object retains excess heat from its common-envelope phase. However, the results of Zorotovic & Schreiber (2022) imply that there may be excess heat in WD0137B's atmosphere. This will be a very interesting result, but it means that the impacts of aging and its formation history are degenerate. I will begin analyzing this object after my paper for ZTF0038B is complete. My first steps will be to follow my ZTF0038 analysis as a blueprint for studying the circulation and evolutionary history of WD0137. I will also be interested to see whether the spectroscopic lightcurves show any peculiar features or asymmetries like I have recently uncovered for ZTF0038.

WD-BD Population Synthesis Paper: From the 5 WD-BDs observed with JWST, I will analyze two of the objects, and other members of our collaboration will analyze the other objects. When all 5 analyses are complete, I would lead a paper that synthesizes all of the findings and provides population-level insights on these systems. I would like to note that a sample size of 5 doesn't sound like a compelling statistical sample for population discussions, but there are only around 15 known WD-BD systems, so our sample is fairly comprehensive. Furthermore, one essential goal of this paper would be to illustrate the importance of WD-BDs in our broader understanding of substellar atmospheres. Although the focus of this paper will depend on the findings of the individual analyses, I would surely discuss the circulation and formation histories of these objects. In fact, I think it would be reasonable to re-run the methods from Zorotovic & Schreiber (2022) using additional age constraints from the JWST data to present updated constraints on $\alpha_{\rm CE}$. I would also be interested in exploring trends among the parameter space including the following observables: total irradiation flux, UV flux, brown dwarf rotation speed, and mass of the brown dwarf. Many of these parameters will be correlated, because brown dwarfs closer to their hosts will tend to receive more total flux, UV flux, and rotate faster.

WD-BDs occupy a unique and unexplored parameter space with respect to these parameters, and I am curious to see how our sample fills this space. We will also have longitudinally-resolved spectra and temperature-pressure profiles across all of the atmospheres. The shapes of these spectra are diverse, and I would be interested to see (at least qualitatively) whether hemispheres with similar T-P profiles also share similar emission features. I am also interested to see if any of these objects show strong signs of excess heat in their atmosphere (as a result of their formation histories). There are many directions that this paper could go, and there is a lot of potential information to share. I anticipate that one of the most important (and perhaps difficult) task will be to decide which angle I find to be the most interesting and informative direction to take the paper.

Acknowledgments

This work is supported by the Virginia Space Grant Consortium Graduate Research fellowship and NASA *JWST* observing support for the *JWST* Cycle 3 GO program 4967.

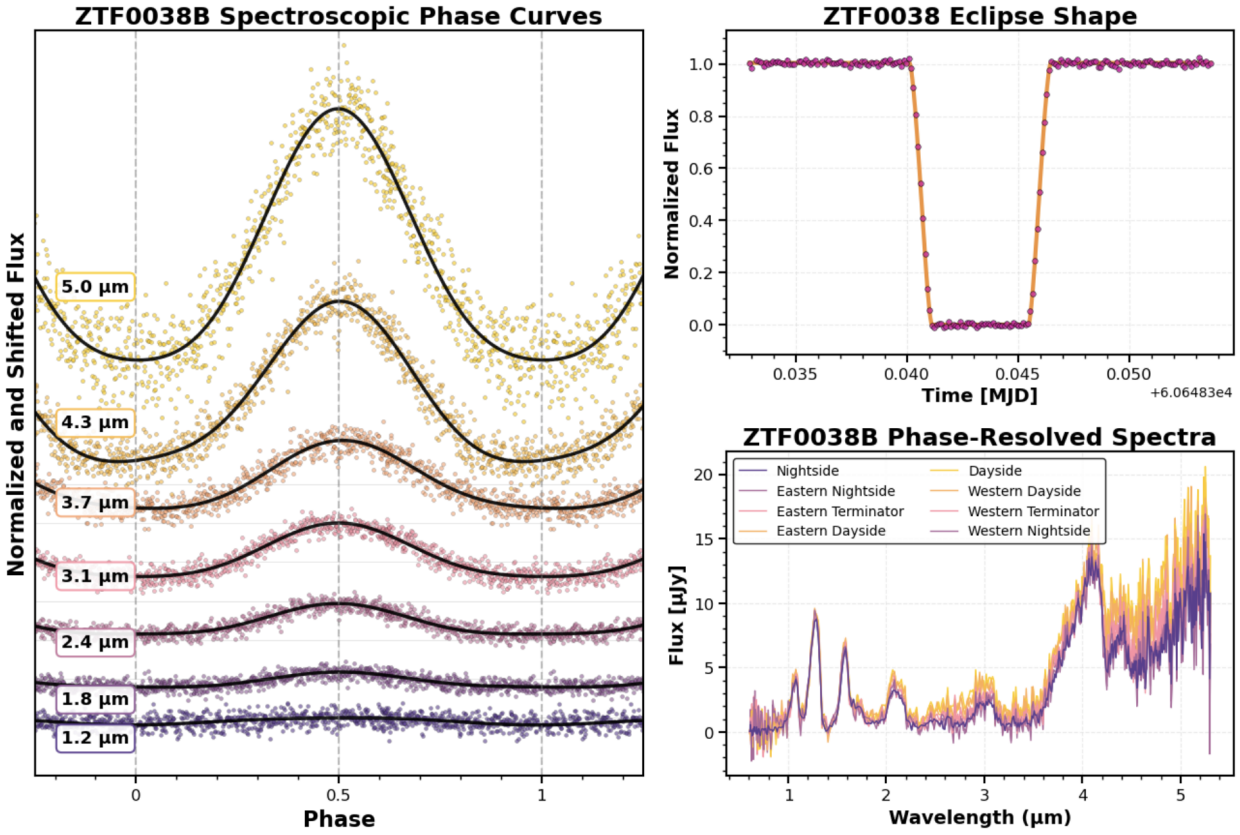

Figure 1: Data products for our phase curve observations of the WD-BD ZTF0038B. **Top:** the phase curves of the the brown dwarf's emission across an entire period. The observed phase modulations are a result of the temperature contrast from the dayside to the nightside. **Center:** the eclipse profile and the eclipse profile fit using `batman` (Kreidberg, 2015). **Bottom:** the brown dwarf emission at 8 phases during the orbit.

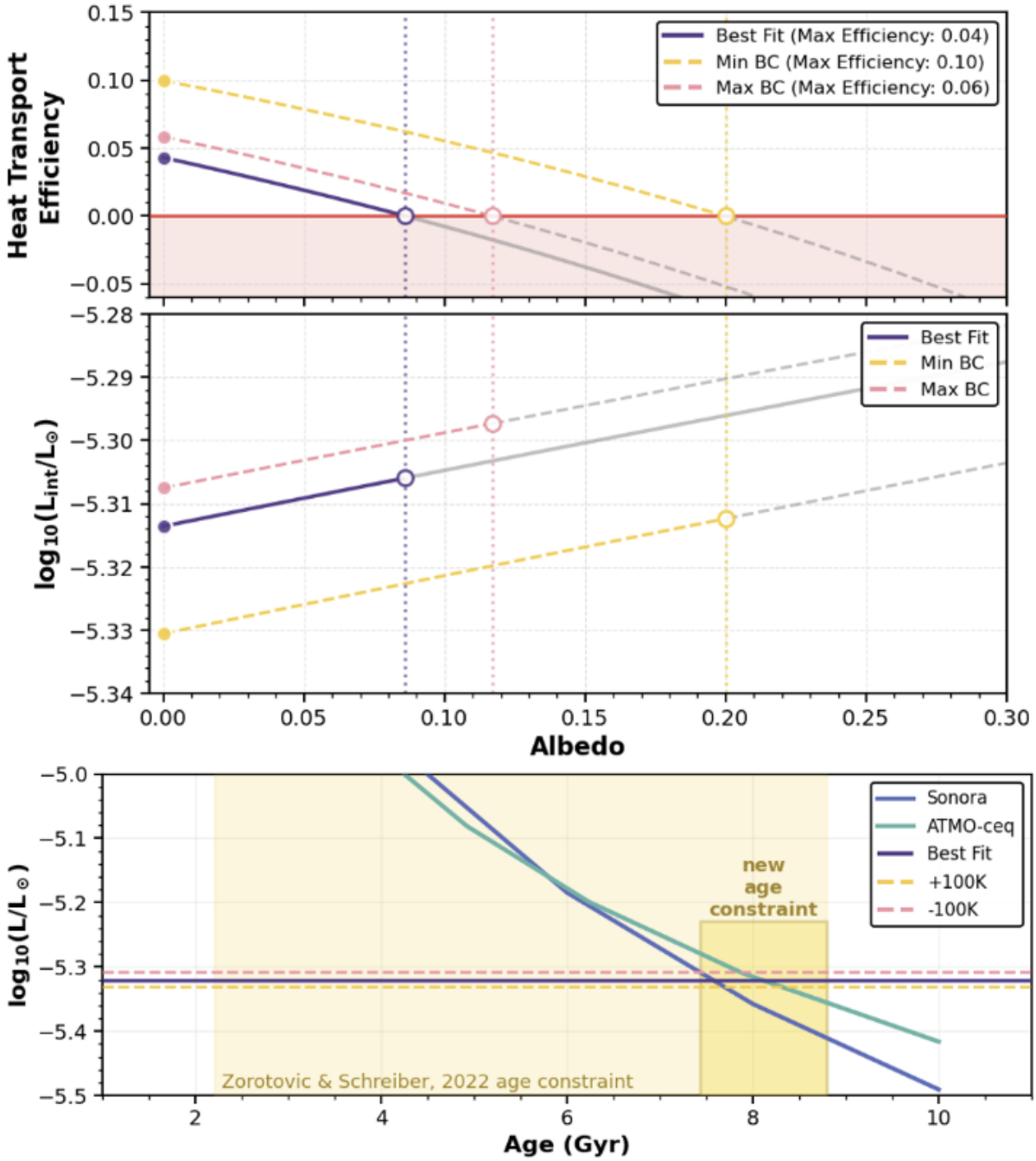

Figure 2: Constraints on bond albedo, heat transfer efficiency, and internal luminosity from energy balance equations. Top: Heat transport efficiency represents the fraction of absorbed dayside heat circulated to the nightside. Negative efficiencies are unphysical; maximum albedo occurs where efficiency reaches zero (open circles, vertical dotted lines). **Center:** Internal luminosity is constrained by the albedo cut-off from the top panel. **Bottom:** Luminosity constraints are compared with isolated brown dwarf evolutionary tracks.

References

Bell, T., Ahrer, E.-M., Brande, J., et al. 2022, The Journal of Open Source Software, 7, 4503, doi: 10.21105/joss.04503

Bushouse, H., Eisenhamer, J., Dencheva, N., et al. 2023, JWST Calibration Pipeline, Zenodo, doi: 10.5281/zenodo.8067394

Kreidberg, L. 2015, Publications of the Astronomical Society of the Pacific, 127, 1161, doi: 10.1086/683602

Marley, M. S., Saumon, D., Visscher, C., et al. 2021, The Astrophysical Journal, 920, 85, doi: 10.3847/1538-4357/ac141d

Mayorga, L. C., Robinson, T. D., Marley, M. S., May, E. M., & Stevenson, K. B. 2021, The Astrophysical Journal, 915, 41, doi: 10.3847/1538-4357/abff50

Splinter, J., Coulombe, L.-P., Frazier, R. C., et al. 2025, Precise Constraints on the Energy Budget of WASP-121 b from its JWST NIRISS/SOSS Phase Curve, arXiv, doi: 10.48550/arXiv.2509.09760

Stolker, T., Quanz, S. P., Todorov, K. O., et al. 2020, Astronomy and Astrophysics, 635, A182, doi: 10.1051/0004-6361/201937159

van Roestel, J., Kupfer, T., Bell, K. J., et al. 2021, The Astrophysical Journal, 919, L26, doi: 10.3847/2041-8213/ac22b7

Zorotovic, M., & Schreiber, M. 2022, Monthly Notices of the Royal Astronomical Society, 513, 3587, doi: 10.1093/mnras/stac1137